

MOL 51581

**The sequence following the signal peptide of the G protein-coupled endothelin B receptor is required for efficient translocation at the endoplasmic reticulum membrane**

**Martina Alken<sup>1,2</sup>, Antje Schmidt<sup>2</sup>, Claudia Rutz, Jens Furkert, Gunnar Kleinau, Walter Rosenthal, and Ralf Schülein**

Leibniz-Institut für Molekulare Pharmakologie, Robert-Rössle-Str. 10, 13125 Berlin, Germany (M.A., C.R., A.S., J.F., G.K., W.R., R.S.) and Bereich Molekulare Pharmakologie und Zellbiologie; Charité - Universitätsmedizin Berlin, Thielallee 71, 14195 Berlin (W.R.)

MOL 51581

**Running title:** ER insertion of the endothelin B receptor

**Corresponding author:** Ralf Schülein, Leibniz-Institut für Molekulare Pharmakologie,  
Robert-Rössle-Str. 10, 13125 Berlin, Germany; Tel: +49 30 94793 255; Fax: +49 30 94793  
109; e-mail: [schuelein@fmp-berlin.de](mailto:schuelein@fmp-berlin.de)

**Number of**

text pages:	34
tables:	0
figures:	10
references:	42
words in the abstract:	203
words in the introduction:	577
words in the discussion:	849

**Abbreviations**

ET<sub>B</sub>R, endothelin B receptor; ET-1, endothelin-1; DMEM, Dulbecco's modified Eagle's medium; EDTA, ethylenediamine tetra-acetate; EndoH, endoglycosidase H; ER, endoplasmic reticulum; ERAD, ER-associated degradation pathway; FRAP, fluorescence recovery after photobleaching; GFP, green fluorescent protein; GPCR, G protein-coupled receptor; LSM, laser scanning microscopy; NYT, N glycosylation acceptor site peptide inhibitor; PAGE, polyacrylamide gel electrophoresis; PBS, phosphate buffered saline; PMSF, phenyl-methylsulfonyl fluoride; PNGaseF, peptide N-glycosidase F; PK; proteinase K; PrP, hamster prion protein; RM, canine pancreatic rough microsomal membranes; ROI, region of interest; RRL, rabbit reticulocyte lysate; SDS, sodium dodecyl sulfate; SP, signal peptide; TX, Triton X-100.

## Abstract

The heptahelical G protein-coupled receptors (GPCRs) must reach their correct subcellular location to exert their function. Receptor domains relevant for receptor trafficking include signal sequences mediating receptor integration into the membrane of the endoplasmic reticulum (ER), and anterograde or retrograde transport signals promoting receptor sorting into the vesicles of the secretory pathway. In addition, receptors must be correctly folded to pass the quality control system of the early secretory pathway. Taking the endothelin B receptor (ET<sub>B</sub>R) as a model, we describe a new type of a transport-relevant GPCR domain. Deletion of this domain (residues Glu<sup>28</sup>-Trp<sup>54</sup>) leads to a fully functional receptor protein which is expressed at a lower level than the wild-type receptor. Subcellular localization experiments and glycosylation state analyses demonstrate that the mutant receptor is neither misfolded, nor retained intracellularly, nor misrouted. Fluorescence recovery after photobleaching (FRAP) analyses demonstrate that constitutive internalisation is also not affected. By using an *in vitro* prion protein targeting assay, we show that this domain is necessary for efficient translocon gating at the ER membrane during early receptor biogenesis. Taken together, we could identify a novel transport-relevant domain in the GPCR protein family. Our data may also be relevant for other GPCRs and unrelated integral membrane proteins.

MOL 51581

G protein-coupled receptors (GPCRs) play an important role in transmembrane signaling and are important drug targets. The GPCRs binding the endothelins (ET-1, ET-2 and ET-3) are important physiological regulators in the vascular system. Two endothelin receptor subtypes are known: the endothelin A receptor (ET<sub>A</sub>R) expressed mainly in vascular smooth muscle cells, and the endothelin B receptor (ET<sub>B</sub>R) expressed mainly in endothelial cells (Arai et al., 1990; Sakurai et al., 1990). Whereas the ET<sub>A</sub>R stimulates G proteins of the G<sub>q/11</sub> and G<sub>12/13</sub> families, the ET<sub>B</sub>R couples to G<sub>i</sub> and G<sub>q/11</sub> (Cramer et al., 2001; Eguchi et al., 1993). The ET<sub>A</sub>R elicits a long-lasting contraction of vascular smooth muscle cells via an increase in cytosolic Ca<sup>2+</sup> concentrations and activation of Rho proteins (Seo et al., 1994; Seko et al., 2003). The ET<sub>B</sub>R stimulates the release of NO and prostacyclin in endothelial cells, thereby causing relaxation of vascular smooth muscle cells (de Nucci et al., 1998).

To accomplish all these functions, GPCRs must be transported along the secretory pathway to their correct location. Several GPCR domains are relevant for intracellular trafficking: i) Signal sequences (von Heijne, 1985; von Heijne, 1990; Higby et al., 2004) are located either at the N terminus of the proteins and cleaved-off following ER translocation (signal peptides), or form part of the mature protein (signal anchor sequence; usually the first transmembrane domain). These sequences mediate integration of the receptors into the membrane of the ER during early receptor biogenesis (Wickner and Schekman, 2005; Osborne et al., 2005). ii) Anterograde or retrograde transport signals may promote receptor sorting into the vesicles of the secretory pathway (Bethune et al., 2006; Gurkan et al., 2006). iii) Some conserved sequences, such as hydrophobic motifs in the C tail, appear to be relevant for a transport-competent folding state (Schülelein et al., 1998; Pankevych et al., 2003). Mutation of these motifs lead to misfolded forms that are retained intracellularly by the quality control system of the early secretory pathway. These proteins are finally subjected to proteolysis by the ER-associated degradation pathway (ERAD) (Schwieger et al., 2008).

MOL 51581

Endothelin receptors belong to the small subgroup of GPCRs possessing cleavable N-terminal signal peptides for ER insertion (Wallin and von Heijne; 1995, Köchl et al., 2002). Similar as for secretory proteins, these signal peptides are recognized shortly after their synthesis by the signal recognition particle (SRP) and mediate the transfer of the nascent chain/SRP/ribosome complex to the translocon complex at the ER membrane (Walter and Johnson, 1994; Shan et al., 2005). Following a GTP-dependent interaction between the SRP and the SRP receptor, the signal peptides and adjacent N tail sequences engage the protein-conducting Sec61 channel of the translocon complex in a hairpin conformation. Accessory components, such as the translocating chain associating membrane protein (TRAM) (Görlich et al., 1992; Görlich and Rapoport, 1993) or the translocon-associated protein (TRAP) complex (Hartmann et al., 1993; Fons et al., 2003) are also involved in signal recognition. The signals then switch the Sec61 channel from the closed to the open configuration thereby mediating not only ER targeting of nascent chains but also translocon gating (Jungnickel et al., 1995; Belin et al., 1996; Osborne et al., 2005).

Whereas the role of signal peptides in translocon gating is well established, the significance of the adjacent N tail sequences following the signal peptide, which also encounter the Sec61 channel, has been unclear. We have addressed this question and show that these residues are necessary for efficient translocon gating in the case of the ET<sub>B</sub>R.

## Materials and Methods

**Materials.** The PrP(A120L) reporter cassette has been described previously (Kim et al., 2002).  $^{125}\text{I}$ -ET-1 (2000 Ci/mmol) was purchased from Amersham Biosciences (Freiburg, Germany). Lipofectamine<sup>TM</sup> 2000 and the vector pSecTag2A were purchased from Invitrogen Life Technologies (Karlsruhe, Germany). The vector plasmid pEGFP-N1 (encoding the red-shifted variant of GFP) and the plasmid pEYFP-Endo were from BD Biosciences Clontech (Mountain View, CA, USA). The transfection reagent FuGENE<sup>TM</sup> HD was from Roche Diagnostics (Mannheim, Germany). DNA-modifying enzymes, PNGaseF and EndoH were from New England Biolabs (Frankfurt am Main, Germany). Oligonucleotides were purchased from Biotex (Berlin, Germany). Trypan blue and Rhodamine 6G were purchased from Seromed (Berlin, Germany). The RotiLoad sample buffer was from Carl Roth (Karlsruhe, Germany). The polyclonal rabbit anti-GFP antiserum 01 (raised against a GST-GFP fusion protein) has been described (Alken et al., 2005). The monoclonal mouse anti-GFP antibody was purchased from Clontech Laboratories (Heidelberg, Germany). Alkaline phosphatase-conjugated anti-mouse IgG was purchased from Dianova (Hamburg, Germany). All other reagents were from Sigma (Taufkirchen, Germany). The materials for the prion protein targeting assay were described previously (Kim et al., 2002).

**DNA manipulations.** Standard DNA manipulations were carried out according to the handbooks of Sambrook and Russel (2001). Nucleotide sequences of the plasmid constructs were verified using the FS Dye Terminator kit from Perkin Elmer (Köln, Germany). Site-directed mutagenesis was carried out with the QuikChange site-directed mutagenesis kit from Stratagene (Heidelberg, Germany).

MOL 51581

**Plasmid constructs.** Constructs used in this study are schematically shown in Fig. 1A. (details of the cloning procedures on request). The sequence of the N tail of the ET<sub>B</sub>R is depicted in Fig. 1B. Full length receptor constructs: Plasmid pET<sub>B</sub>.GFP encodes the ET<sub>B</sub>R in the vector plasmid pEGFP-N1 (Oksche et al., 2000). The receptor is C-terminally tagged with a GFP moiety (thereby deleting the stop codon of the receptor). In plasmid pET<sub>B</sub>.Δ27.GFP, the sequence Glu<sup>28</sup>-Trp<sup>54</sup> (27 residues) of the mature N-tail of the ET<sub>B</sub>R was deleted. For the construction of plasmid ET<sub>B</sub>Ins.GFP, the sequence encoding Glu<sup>28</sup>-Trp<sup>54</sup> was deleted from ET<sub>B</sub>R.GFP and reinserted between the codons for Pro<sup>81</sup> and Pro<sup>82</sup>. Marker protein fusions: Plasmid ET<sub>B</sub>.SP.PrP encodes an N-terminal fusion of the signal peptide (Met<sup>1</sup>-Gly<sup>26</sup>) of the ET<sub>B</sub>R to the hamster prion protein marker cassette PrP(A120L) (Kim et al., 2002). In plasmid ET<sub>B</sub>.SP28.PrP residues Glu<sup>27</sup>-Trp<sup>54</sup> (28 residues) were added C-terminal of the signal peptide thereby replacing 28 amino acid residues of the PrP sequence.

**Cell culture and transfection.** Cells were cultured at 37 °C and 5 % CO<sub>2</sub>. HEK 293 cells were grown in Dulbecco's modified Eagle's medium (DMEM) containing 10 % (v/v) fetal calf serum (FCS), penicillin (100 U/ml) and streptomycin (100 μg/ml). Transfection of the cells with plasmids and Lipofectamine<sup>TM</sup> 2000 or FuGENE<sup>TM</sup> HD was carried out according to the supplier's recommendations. Equal amounts of plasmid were transfected in each experiment to allow comparison of the receptor expression levels.

**Confocal laser scanning microscopy.** HEK 293 cells (2.5 x 10<sup>5</sup>) grown for 24 h in a 35 mm diameter dish containing a poly-L-lysine-coated cover slip were transfected with 1 μg plasmid DNA and FuGENE<sup>TM</sup> HD according to the supplier's recommendations. Cells were incubated overnight, washed once with PBS and transferred immediately into a self-made chamber (details on request).

MOL 51581

For the colocalization of the receptor GFP signals with plasma membrane Trypan blue signals (Schülein et al., 1998), live cells were covered with 1 ml PBS, and Trypan blue was added to a final concentration of 0.05 %. After 1 min of staining, GFP and Trypan blue signals were visualized at room temperature using a Zeiss LSM510-META invert confocal laser-scanning microscope (objective lens: 100x/1.3 oil; optical section: <0.9  $\mu\text{m}$ ; multitrack mode; GFP,  $\lambda_{\text{exc}}$ : 488 nm, argon laser, BP filter: 500-530 nm; Trypan blue,  $\lambda_{\text{exc}}$ : 543 nm, HeNe laser, LP filter: 560 nm). The overlay of both signals was computed using the Zeiss LSM510 software (release 3.2; Carl Zeiss AG, Jena, Germany). Images were imported into Photoshop software (release 6.0; Adobe Systems Inc., San Jose, CA, USA), and contrast was adjusted to approximate the original image.

To quantify GFP signals, the signal intensities at the plasma membrane and in the cell's interior were measured using the 8 Bit grey scale (ranging from 0 to 250) provided by the LSM510 software. Total GFP fluorescence intensity of cells (n= 16-27 cells) or the ratio of plasma membrane and intracellular signals were determined.

For Rhodamine 6G staining of the ER (Schülein et al., 1998), live cells expressing the receptor constructs were washed with PBS, and incubated for 40 min with 50 nM Rhodamine 6G in PBS. The receptor GFP signals and the ER Rhodamine 6G signals were analysed by confocal LSM (objective lens: 100x/1.3 oil; optical section: <0.9  $\mu\text{m}$ ; multitrack mode; GFP,  $\lambda_{\text{exc}}$ : 488 nm, argon laser, BP filter: 494-516 nm; Rhodamine 6G,  $\lambda_{\text{exc}}$ : 543 nm, HeNe laser, LP filter: 560 nm) and processed as described above.

For FRAP experiments, a maximal laser intensity ( $\lambda_{\text{exc}} = 488 \text{ nm}$ ) with 50 iterations was used to bleach the selected ROIs in the cells. Images were recorded in a time series of 1650 s with an interval of 150 s (only the pictures after 0, 150, 300, 900 and 1650 s are shown). Live cell imaging of GFP fluorescence signals and image processing were performed as described above. Fluorescence measurements in the ROIs and statistical analyses (n = 6-8 cells) were



MOL 51581

performed using the 8 Bit grey scale of the LSM510 software. Mean values were fitted using the software GraphPad Prism (release 3.02; La Jolla, CA, USA) and the equation  $I(t) = \text{Max} + (\text{Min} - \text{Max}) \times \exp(-t/T)$ . Mean values were expressed in percent of the initial value.

**Northern blot.** The experiment was carried out essentially as described previously (Alken et al., 2005). Total RNA was isolated from transiently transfected HEK 293 cells and Northern blot analysis (30  $\mu\text{g}$  of RNA/lane) was performed with  $^{32}\text{P}$ -labeled ET<sub>B</sub>.GFP cDNA. Blots were stripped and reprobed with a  $^{32}\text{P}$ -labeled cDNA fragment specific for actin. Untransfected cells were used as a control.

**Pharmacological methods.** [ $^{125}\text{I}$ ]ET-1 binding assay. The experiment was carried out with intact transiently transfected HEK 293 cells ( $1.8 \times 10^4$ ) grown on Poly-L-Lysine-coated 96 well plates. Cells were washed twice with 100  $\mu\text{l}$  of binding buffer consisting of PBS-I (0.9 mM CaCl<sub>2</sub>, 0.5 mM MgCl<sub>2</sub>, 2.7 mM KCl, 136.9 mM NaCl, 1.5 mM KH<sub>2</sub>PO<sub>4</sub>, 8.1 mM Na<sub>2</sub>HPO<sub>4</sub>, 0.5 mM PMSF, 0.5 mM benzamidine, 3,2  $\mu\text{g}/\text{ml}$  trypsin inhibitor, 1.4  $\mu\text{g}/\text{ml}$  aprotinin, 0.2 mg/ml bacitracin, 0.05% BSA, pH 7.4). [ $^{125}\text{I}$ ]ET-1, diluted in 100  $\mu\text{l}$  of the same buffer, was added to achieve the indicated concentrations. Nonspecific binding was determined in the presence of 1  $\mu\text{M}$  unlabeled ET-1. Cells were incubated with the ligand for 2 h on ice (to avoid receptor internalization), washed quickly two times with ice-cold PBS-I and lysed with 100  $\mu\text{l}$  0.1 N NaOH. The lysate was transferred to tubes and radioactivity was measured using a  $\gamma$ -counter. Inositol phosphate accumulation assay. The experiment was carried out with intact transiently transfected HEK 293 cells as described previously for stably transfected HEK 293 cells (Wietfeld et al., 2004). All data were analyzed using the GraphPad Prism software (release 3.02; La Jolla, CA, USA).

MOL 51581

**Immunoprecipitation of GFP-tagged ET<sub>B</sub>R deletion constructs and immunoblotting.**

HEK 293 cells ( $4 \times 10^6$ ), grown on 100 mm diameter dishes were transiently transfected with 10  $\mu$ g plasmid DNA and FuGENE<sup>TM</sup> HD according to the supplier's recommendations. Cells were cultivated for 24 h, washed twice with PBS (pH 7.4) and lysed for 1 h with 1 ml of lysis buffer (50 mM Tris-HCl, 150 mM NaCl, 1 mM EDTA, 0.1 % (w/v) SDS, 1 % (v/v) Triton X-100, pH 8.0, supplemented with 0.5 mM PMSF, 0.5 mM benzamidine, 1.4  $\mu$ g/ml aprotinin, 3.2  $\mu$ g/ml trypsin inhibitor). Insoluble debris was removed by centrifugation (20 min, 13,000 x g). The supernatant was supplemented with polyclonal rabbit anti-GFP antiserum 01 coupled to protein A sepharose Cl-4B beads and the sample was incubated over night (beads were prepared by equilibrating 10 mg of the beads with lysis buffer and subsequent over night incubation with 2  $\mu$ l polyclonal rabbit anti-GFP antiserum 01). GFP-tagged receptors were precipitated (2 min, 700 x g), and the beads were washed twice with 2 ml of washing buffer 1 (50 mM Tris-HCl, 500 mM NaCl, 1 mM EDTA, 0.1 % (w/v) SDS, 0.5 % (v/v) Triton X-100, pH 8.0) and once with 2 ml of washing buffer 2 (50 mM Tris-HCl, 1 mM EDTA, 0.1 % (w/v) SDS, 1 % (v/v) Triton X-100, pH 7.4). Precipitated receptors were treated with EndoH or PNGaseF according to the supplier's recommendations or left untreated. Samples were supplemented with RotiLoad sample buffer, incubated for 5 min at 95 °C, and analyzed by SDS-PAGE/immunoblotting (10 % SDS) using a monoclonal mouse anti-GFP antibody and alkaline phosphatase-conjugated anti-mouse IgG. Immunoblots were carried out as described (Kyhse-Andersen, 1984).

**Prion protein targeting assay.** *In vitro* transcription with SP6 RNA polymerase was performed for 1 h at 40 °C. Translation with rabbit reticulocyte lysate in the presence of [<sup>35</sup>S] methionine, and translocation into canine rough microsomal membranes were carried out at 40 °C for 40 min as described previously (Kim et al., 2001; Kim et al., 2002). Proteinase K

MOL 51581

(PK) digestion (0.5 mg/ml) was performed for 60 min at 0 °C; reactions were terminated with 5 mM PMSF. The N glycosylation acceptor site inhibitor peptide NYT (peptide sequence = NH<sub>2</sub>-Asp-Tyr-Thr-COOH) was used in a concentration of 160 μM in all samples to inhibit N glycosylation of the prion protein moieties thereby facilitating interpretation of the results. Triton X-100 (TX) (1 %) was used to permeabilize membranes. All samples were transferred into 10 volumes of a preheated solution containing 1% SDS and 0.1 M Tris-HCl (pH 8.0) and analyzed by SDS-PAGE on 12 % Tris/Tricine gels. Proteins were visualized by autoradiography.

## Results

**Deletion of the sequence Glu<sup>28</sup>-Trp<sup>54</sup> decreases ET<sub>B</sub>R expression without causing misfolding, intracellular retention, misrouting or increased constitutive internalization of the receptor.** We used the previously described GFP-tagged construct ET<sub>B</sub>.GFP for our work (Fig. 1A; the GFP tag does not influence the pharmacological or trafficking properties of the receptor; Oksche et al., 2000). To study the significance of the sequence following the signal peptide for receptor trafficking, a deletion mutant was constructed by eliminating the sequence encoding residues Glu<sup>28</sup>-Trp<sup>54</sup> (Fig. 1A, construct ET<sub>B</sub>Δ27.GFP; see Fig. 1B for the N tail sequence of the ET<sub>B</sub>R).

To preclude an influence of the deletion on mRNA synthesis, a Northern blot analysis with total RNA derived from transiently transfected HEK 293 cells was performed (Fig. 2). For ET<sub>B</sub>.GFP and ET<sub>B</sub>Δ27.GFP, RNA bands of 2.0 kb and 1.9 kb were detected respectively (the smaller size in the case of mutant ET<sub>B</sub>Δ27.GFP is due to the deletion). Both transcripts were present in similar amounts demonstrating that the deletion has no influence on mRNA synthesis and stability.

We next compared the pharmacological properties of the constructs ET<sub>B</sub>.GFP and ET<sub>B</sub>Δ27.GFP. HEK 293 cells were transiently transfected and [<sup>125</sup>I]ET-1-binding profiles of intact cells were recorded (Fig. 3A). The K<sub>D</sub> values of ET<sub>B</sub>.GFP and ET<sub>B</sub>Δ27.GFP were almost identical (0.14±0.02 nM vs. 0.13±0.02 nM respectively) demonstrating that the deletion of Glu<sup>28</sup>-Trp<sup>54</sup> does not influence the ligand binding properties of the receptor. Maximal binding of ET<sub>B</sub>Δ27.GFP, however, was substantially reduced to 45 % of the wild type level (B<sub>max</sub> values: 84.5±9.2 fmol/mg for ET<sub>B</sub>.GFP vs. 38.1±4.9 fmol/mg for ET<sub>B</sub>Δ27.GFP). The decreased B<sub>max</sub> value of ET<sub>B</sub>Δ27.GFP together with the maintained K<sub>D</sub> value indicate that less functional receptors are present at the plasma membrane in the case of

MOL 51581

ET<sub>B</sub>Δ27.GFP. Measuring ET-1-induced inositol phosphate accumulation in transiently transfected HEK 293 cells yielded similar dose response curves for ET<sub>B</sub>.GFP and ET<sub>B</sub>Δ27.GFP (Fig. 3B). The EC<sub>50</sub> values were 4.5±0.1 nM for ET<sub>B</sub>.GFP vs. 3.3±0.1 nM for ET<sub>B</sub>Δ27.GFP indicating that the deletion mutant has normal signaling properties. The decreased number of ET<sub>B</sub>Δ27.GFP receptors is nevertheless sufficient to achieve almost maximal adenylyl cyclase stimulation due to a receptor reserve in the transfected cells. Taken together these results demonstrate that the Glu<sup>28</sup>-Trp<sup>54</sup> deletion does not influence the pharmacological properties of the ET<sub>B</sub>R but decreases receptor expression at the plasma membrane.

Deletion of the Glu<sup>28</sup>-Trp<sup>54</sup> sequence does not involve the signal peptide itself. It is also unlikely that the deletion affects a transport signal since these are located in intracellular domains of integral membrane proteins allowing direct or indirect binding of vesicular coat components. Although the K<sub>D</sub> and EC<sub>50</sub> values of the mutant ET<sub>B</sub>Δ27.GFP are similar to those of the wild-type indicating that the mutant receptor is correctly folded, the deletion may nevertheless lead to a subtle change in receptor conformation which may be recognized by the quality control system of the ER and/or other components of the early secretory pathway. In this case, the mutant receptor would be initially retained in the early secretory pathway and finally subjected to proteolysis by the ER-associated degradation pathway (ERAD) (Schwieger et al., 2008). Such a behaviour of mutant ET<sub>B</sub>Δ27.GFP may explain the decreased number of receptors at the plasma membrane. GPCR retention in the early secretory pathway and subsequent degradation by the ERAD is accompanied by a decrease in the ratio of complex and high mannose-glycosylated receptors (e.g. Schülein et al., 1998; Robben et al., 2005; Schwieger et al., 2008); the complex-glycosylated forms representing the mature receptors and the high mannose forms the immature forms present in the early secretory pathway.

MOL 51581

To address for changes in steady state glycosylation, ET<sub>B</sub>Δ27.GFP and ET<sub>B</sub>.GFP were immunoprecipitated from lysates of transiently transfected HEK 293 cells. Receptors were treated by EndoH (removing only high mannose glycosylations) or PNGaseF (removing both high mannose and complex glycosylations) and detected by immunoblotting. The same two protein bands were detectable for ET<sub>B</sub>.GFP and ET<sub>B</sub>Δ27.GFP. (Fig. 4 “a” and “b”). The stronger upper bands (“a”) represent the mature, complex-glycosylated forms of the receptors since they were resistant to EndoH treatment. The lower, barely detectable bands (“b”) represent immature high mannose forms and/or nonglycosylated forms (these two forms can not be distinguished following PNGaseF treatment because of their small mass differences). The apparent molecular masses of the protein bands following PNGaseF treatment are in good agreement with the calculated molecular masses of the constructs (calculated = 77.16 kDa for ET<sub>B</sub>.GFP and 74.11 kDa for ET<sub>B</sub>Δ27.GFP). Except of the size difference due to the deletion, the protein pattern of ET<sub>B</sub>.GFP and ET<sub>B</sub>Δ27.GFP was very similar and densitometric measurements revealed a similar ratio of complex-glycosylated and high mannose/nonglycosylated forms (8.0 for ET<sub>B</sub>.GFP and 7.0 for ET<sub>B</sub>Δ27.GFP). However, the total amount of protein of ET<sub>B</sub>Δ27.GFP (sum of high mannose/nonglycosylated and complex-glycosylated forms) was decreased to 28 % of that of ET<sub>B</sub>.GFP. Consistent with the ligand binding experiments, these results indicate that deletion of the sequence Glu<sup>28</sup>-Trp<sup>54</sup> decreases expression of the ET<sub>B</sub>R without causing receptor misfolding and a subsequent increase in intracellular retention and degradation by the ERAD.

To confirm these results we performed limited proteolysis experiments using transiently transfected HEK 293 cells expressing ET<sub>B</sub>.GFP and ET<sub>B</sub>Δ27.GFP. Receptors were treated with increasing amounts of trypsin, and the precipitated degradation products were detected by immunoblotting. The same pattern of protein bands was detected for ET<sub>B</sub>.GFP and

MOL 51581

ET<sub>B</sub>Δ27.GFP consistent with the view that receptor folding is not affected by the Glu<sup>28</sup>-Trp<sup>54</sup> deletion (data not shown).

Retention of a mutant receptor by the quality control system and subsequent degradation by the ERAD is also accompanied by a steady state accumulation of the receptor in the early secretory pathway which is detectable microscopically (e.g. Schülein et al., 1998; Robben et al., 2005; Schwieger et al., 2008). To confirm the results that ET<sub>B</sub>Δ27.GFP is not subjected to a more stringent quality control in the early secretory pathway, we analyzed the subcellular location of the GFP signals of the receptor by confocal LSM and assessed their colocalization with the plasma membrane dye Trypan blue (Fig. 5A, upper panel) (Schülein et al., 1998) or the ER dye Rhodamine 6G (Fig. 5A, lower panel) (Schülein et al., 1998) in transiently transfected HEK 293 cells. In the case of a folding defect causing receptor retention and subsequent ERAD degradation, a decrease in the amount of plasma membrane receptors should lead to a concomitant increase in the amount of receptors colocalizing with the ER marker (Schülein et al., 1998). Analysis of the GFP signals of the constructs revealed a significantly reduced overall expression of ET<sub>B</sub>Δ27.GFP in comparison to ET<sub>B</sub>.GFP. However, the subcellular distribution of ET<sub>B</sub>Δ27.GFP and ET<sub>B</sub>.GFP was similar and no increase in Rhodamine 6G colocalization was observed for ET<sub>B</sub>Δ27.GFP. In addition, we have quantified and statistically analyzed the GFP signals of ET<sub>B</sub>Δ27.GFP and ET<sub>B</sub>.GFP. The total fluorescence, i.e. the sum of intracellular and plasma membrane signals, was significantly reduced in the case of ET<sub>B</sub>Δ27.GFP, demonstrating a decrease in receptor expression to 38 % of the wild type level (Fig. 5B, left panel). The ratio of intracellular and plasma membrane fluorescence, however, was unchanged again demonstrating that retention of the mutant in the early secretory pathway is not increased (Fig. 5B, right panel). These data are entirely consistent with the pharmacological data, glycosylation state analyses and limited proteolysis experiments.

MOL 51581

The reduced amount of cell surface receptors in the case of ET<sub>B</sub>Δ27.GFP may also result from an increase in constitutive internalisation (removal from the cell surface without ligand stimulation). To address this question, we performed FRAP experiments with transiently transfected HEK 293 cells expressing ET<sub>B</sub>Δ27.GFP and ET<sub>B</sub>.GFP. Endosomal compartments of the cells containing receptors were identified by colocalizing the receptor's GFP signals with those of the cotransfected endosomal marker protein pEYFP-Endo (data not shown). ROIs were selected by confocal LSM and the endosomal compartments were bleached with maximal laser intensity (Fig. 6A). Refilling of the ROIs with receptor GFP signals was recorded in a time series of 1600 s with an interval of 150 s (only the pictures after 0, 150, 300, 900 and 1650 s are shown in Fig. 6A). Quantification of the time-dependent refilling of the photobleached endosomal compartments yielded almost identical curves for ET<sub>B</sub>Δ27.GFP and ET<sub>B</sub>.GFP demonstrating that constitutive internalisation of the mutant is not affected by the mutation.

Taken together, deletion of residues Glu<sup>28</sup>-Trp<sup>54</sup> of the ET<sub>B</sub>R decreases overall receptor expression substantially. Neither receptor misfolding, increased retention/ERAD degradation, misrouting nor an increased constitutive internalization was detectable. Thus, our data indicate that the Glu<sup>28</sup>-Trp<sup>54</sup> sequence facilitates, like the signal peptide itself, an early step in receptor biogenesis such as translocon gating. Such a function is reasonable, since the sequence following the signal peptide also encounters the Sec61 channel during the hairpin insertion mechanism.

**The sequence Glu<sup>28</sup>-Trp<sup>54</sup> of the N tail of the ET<sub>B</sub>R is required for efficient translocon gating.** Recently, an efficient method was described for secretory proteins to measure the translocon gating properties of their signal peptides, and consequently that of adjacent sequences, using the PrP(A120L) protein as a marker (Kim et al., 2001; Kim et al., 2002). The



MOL 51581

PrP(A120L) reporter is a modified version of the PrP hamster prion protein lacking its N-terminal signal peptide (Fig. 7A). The remaining single hydrophobic transmembrane domain of this construct is unable to mediate ER targeting, making efficient translocation of the protein at the ER membrane dependent on the introduction of a signal peptide. In this system, [<sup>35</sup>S] methionine-labeled fusion proteins are synthesized in the presence of canine pancreatic rough microsomal membranes (RMs) using an *in vitro* rabbit reticulocyte lysate translation system. Nascent chains containing signal peptides failing to target to the ER membrane and/or failing to promote binding to the translocon result in exclusive cytosolic and completely PK-sensitive translation products (Fig. 7A, step 1). In contrast, signal peptides targeting the nascent chains to the translocon lead to the integration of the fusion proteins into the ER membrane (Fig. 7A, step 2). Two different orientations of the fusions are possible dependent on the gating properties of the signal peptide: if the signal peptide initiates the access to the luminal environment efficiently, the N<sub>tm</sub> form (Fig. 7A, step 3.1, = N<sub>exo</sub>-C<sub>cyt</sub> form) of the construct is synthesized and the signal peptide is cleaved-off after translocation. Complete translocation of the construct into the ER lumen may also take place in this case (Fig. 7A; step 3.1, Lu form). If, however the signal peptide opens the translocon inefficiently, the TM of the PrP(A120L) reporter takes over the gating function, and the C<sub>tm</sub> form (Fig. 7A, step 3.2, = N<sub>cyt</sub>-C<sub>exo</sub> form) with an uncleaved signal peptide is synthesized. N<sub>tm</sub> or C<sub>tm</sub> forms can be distinguished by a protease protection assay, the resulting N<sub>tm</sub> fragment being smaller than the C<sub>tm</sub> fragment.

To address the question of whether the sequence following the signal peptide of the ET<sub>B</sub>R facilitates translocon gating, we have introduced the signal peptide of the ET<sub>B</sub>R alone and together with its adjacent Glu<sup>27</sup>-Trp<sup>54</sup> sequence into the PrP(A120L) marker protein, thereby replacing the original PrP sequences (Fig. 1A; constructs ET<sub>B</sub>.SP.PrP and ET<sub>B</sub>.SP28.Pr, respectively). The total number of amino acids remained constant in each construct. *In vitro*

MOL 51581

synthesis of the ET<sub>B</sub>.SP.PrP construct in the presence of RMs led mainly to the formation of one major protein band on the gel after autoradiography, representing the Ctm form of the construct with its uncleaved signal peptide (Fig. 7B, lane 1, “Ctm”; see the lower panel of Fig. 7B for the interpretation of the results). The fact that this band represents the Ctm form could be concluded from the apparent molecular mass of the resulting fragment in the PK protection assay (Fig. 7B, lane 3, “Ctm-d”; see also Kim et al., 2002).

If the adjacent Glu<sup>27</sup>-Trp<sup>54</sup> sequence of the ET<sub>B</sub>R is additionally fused (replacing 28 residues of PrP; construct ET<sub>B</sub>.SP28.PrP; see Fig. 1A), different results are obtained. *In vitro* synthesis in the presence of RMs yields two bands (Fig. 7B, lane 2). The lower, stronger band represents both the mature Ntm form (“Ntm”) and the translocated luminal (“Lu”) form sharing the same apparent molecular mass. The upper faint band represents the precursor (“Pre”) of both the Ntm and luminal forms still possessing the signal peptide (this band is detectable in variable amounts from experiment to experiment and was omitted in the interpretation of the results in the lower panel of Fig. 7B). The identity of Lu and Ntm forms could again be derived from the PK protection assay, the Lu form being completely resistant to PK digestion, the Ntm form being digested to the corresponding low molecular mass fragment (Fig. 7B, lane 4, “Ntm-d”; compare to the Ctm-d fragment of ET<sub>B</sub>SP.PrP, lane 3; see also Kim et al., 2002).

Taken together, the presence of the ET<sub>B</sub>.SP.PrP construct in its Ctm form in the RMs demonstrates that the signal peptide of the ET<sub>B</sub>R alone is sufficient for ER targeting, but not for efficient translocon gating. Only if the Glu<sup>28</sup>-Trp<sup>54</sup> sequence of the ET<sub>B</sub>R is additionally present, Ntm and Lu forms indicating efficient translocon opening are detectable.

The recently published structure of the canine Sec61 protein (Ménétre et al. 2008) revealed the presence of a 22 Å wide cavity in the closed conformation of the protein-conducting channel. When a helical structure model of the signal peptide of the ET<sub>B</sub>R (26 amino acids) is

MOL 51581

inserted into this cavity above the channel-sealing plug domain (Fig. 8), it is obvious that the channel may not only incorporate the signal peptide and an adjacent domain of similar length which may help to gate the channel, but also additional sequences. This raises the question of whether the Glu<sup>28</sup>-Trp<sup>54</sup> sequence must directly follow the signal peptide or whether it may be located more C-terminally. To address this question, we deleted the Glu<sup>28</sup>-Trp<sup>54</sup> sequence of ET<sub>B</sub>R.GFP and reinserted it between residues Pro<sup>81</sup> and Pro<sup>82</sup> by site directed mutagenesis (resulting mutant ET<sub>B</sub>Ins.GFP; see Fig. 1). [<sup>125</sup>I]ET-1 binding experiments under saturating conditions using transiently transfected HEK 293 cells indicate almost wild type binding properties for this mutant, in contrast to mutant ET<sub>B</sub>Δ27.GFP (Fig. 9A). Colocalization the receptor's GFP signals with the plasma membrane marker Trypan blue by confocal LSM (Fig. 9B) and quantification of the membrane-bound GFP signals (Fig. 9C) also show that expression of ET<sub>B</sub>Ins.GFP is close to that of the wild-type. These results were confirmed by immunoprecipitation/immunoblotting experiments and by FACS quantification of the GFP fluorescence signals (data not shown). Taken together, these results indicate that mutant ET<sub>B</sub>Ins.GFP has almost wild-type gating properties. Thus, the Glu<sup>28</sup>-Trp<sup>54</sup> sequence must not directly follow the signal peptide to exert its function.

## Discussion

Our experiments with transfected cells demonstrated that deletion of the sequence Glu<sup>28</sup>-Trp<sup>54</sup> of the ET<sub>B</sub>R decreases overall receptor expression substantially. Neither receptor misfolding, increased retention/ERAD degradation, misrouting nor an increased constitutive internalization was detectable. Using the *in vitro* PrP targeting assay, we could directly show that this domain facilitates translocon gating at the ER membrane. Thus, we have identified a novel transport-relevant domain in the GPCR family.

In the prion protein targeting assay, the signal peptide of the ET<sub>B</sub>R could only mediate targeting of the nascent chain/ribosome/SRP complex to the membrane and the Glu<sup>28</sup>-Trp<sup>54</sup> sequence was a requirement for translocon gating (compare orientations of constructs ET<sub>B</sub>.SP.PrP vs. ET<sub>B</sub>.SP28.PrP, Fig. 7). In the case of the full length receptor constructs, ET<sub>B</sub>R expression was only improved if the Glu<sup>28</sup>-Trp<sup>54</sup> sequence was located adjacent to the signal peptide, albeit significantly (compare ET<sub>B</sub>.GFP vs. ET<sub>B</sub>Δ27.GFP in the binding experiments, glycosylation state analyses and confocal LSM microscopy; Figs. 3, 4 and 5 respectively). These results could be interpreted by a basal gating efficiency of the signal peptide alone in living transfected cells but not in the *in vitro* prion protein targeting assay leading to a stricter requirement of the Glu<sup>28</sup>-Trp<sup>54</sup> sequence in the *in vitro* system. More likely, however, the different sequences following the signal peptide in each of the constructs may stimulate signal peptide-mediated gating differently: the best gating efficiency is observed when the signal peptide of the ET<sub>B</sub>R encounters its original Glu<sup>28</sup>-Trp<sup>54</sup> sequence, either in full length constructs or in PrP fusions (constructs ET<sub>B</sub>.GFP and ET<sub>B</sub>.SP28.PrP respectively). Gating is possible but decreased when the Glu<sup>28</sup>-Trp<sup>54</sup> sequence is deleted and replaced by the P55-P82 sequence of the ET<sub>B</sub>R (full length construct ET<sub>B</sub>Δ27.GFP). Gating is completely prevented when the signal peptide is fused directly to a PrP sequence (construct ET<sub>B</sub>.PrP). In

MOL 51581

conclusion, the gating properties of the signal peptide seem to be functionally linked to the adjacent N tail sequence of the mature proteins.

A similar protein specific match of signal peptide and mature domain functions has recently been proposed for secretory proteins (Kim et al., 2002). In these studies, signal peptide-mediated gating was also related to the adjacent sequences and decreased upon exchange of the original mature domain although the size of the domain responsible for this effect had not been determined (Kim et al., 2002). Our results indicate that the same applies to the ET<sub>B</sub>R and potentially to other GPCRs and integral membrane proteins possessing cleavable signal peptides. Taking the data for secretory proteins and our results together, it may be speculated that signal peptides and their adjacent sequences represent functional units, allowing efficient translocon gating only in the original combination.

The mechanism by which the Glu<sup>28</sup>-Trp<sup>54</sup> sequence of the ET<sub>B</sub>R facilitates translocon gating remains elusive. Signal peptide-mediated relocation of the plug domain occluding the Sec61 channel (van den Berg et al., 2004) may be facilitated by an associated, or, in contrast, by a non-associated combination of signal peptide and assisting sequence when encountering the channel in a hairpin mechanism (Fig. 10 “a” and “b” respectively). Interactions of Glu<sup>28</sup>-Trp<sup>54</sup> with the TRAP complex may also play a role since it has been shown that this complex is involved in signal peptide-mediated translocon gating, at least in the case of some signal peptides (Fons et al., 2003). The expression data of mutant ET<sub>B</sub>Ins.GFP (Fig. 9) indicate, that a domain assisting in translocon gating must not directly follow the signal peptide. Taking the spatial dimensions within the Sec61 channel into account (Fig. 8), it is obvious that its cavity can also accept assisting domains which are located more C-terminally consequently forming larger hairpin structures.

Our data also raise the question whether the Glu<sup>28</sup>-Trp<sup>54</sup> sequence represents a conserved domain in the GPCR protein family. Signal peptides of different proteins have a common

MOL 51581

secondary structure but no sequence homologies (von Hejne, 1985; von Heijne, 1990). Thus, if signal peptides and assisting N tail sequences form indeed a functional unit during translocon gating, it is unlikely that the respective N-tail sequences have sequence homologies. In agreement with this view, we did not find sequences in the N tails of GPCRs which are homologous to the Glu<sup>28</sup>-Trp<sup>54</sup> sequence (data not shown).

The structural analysis of GPCRs is an important and difficult task and it has been frequently tried to increase GPCR expression by the fusion of signal peptides, in particular in the case of those GPCRs that do normally contain uncleaved signal anchor sequences (e.g. Guan et al., 1992; Grisshammer et al., 1993, Grünewald et al., 1996; Kempf et al., 2002). However, the outcome of these experiments was not predictable and signal peptide-mediated increase in expression was not obtained regularly. Taking our data into account, it is conceivable that an increase in expression might only be achieved when a signal peptide is fused to an N tail domain matching the requirements of the signal peptide. Another conclusion from our data is that care should be taken when GPCRs possessing signal peptides are modified in their extreme N tail, for example by fusing tags to facilitate protein detection, since these modifications may have a strong impact on protein expression.

MOL 51581

## **Acknowledgments**

We thank Ramanujan Hegde (NIH, Bethesda, USA) for help in preparing the prion protein targeting assay. We thank Marta Szaszak and Burkhard Wiesner for useful discussions. We would like to thank Gisela Papsdorf of the cell culture facilities of the Leibniz-Institut für Molekulare Pharmakologie and Erhard Klausenz from the DNA sequencing service group for their contributions. We also thank Jenny Eichhorst for excellent technical assistance.

## References

Alken M, Rutz C, Köchl R, Donalies U, Oueslati M, Furkert J, Wietfeld D, Hermosilla R, Scholz A, Beyermann M, Rosenthal W and Schüle R (2005) The signal peptide of the rat corticotropin-releasing factor receptor 1 promotes receptor expression but is not essential for establishing a functional receptor. *Biochem J* **390**:455-464.

Arai H, Hori S, Aramori I, Ohkubo H and Nakanishi S (1990) Cloning and expression of a cDNA encoding an endothelin receptor. *Nature* **348**:730-732.

Belin D, Bost S, Vassalli JD and Strub K (1996) A two-step recognition of signal sequences determines the translocation efficiency of proteins. *EMBO J* **15**:468-478.

Bethune J, Wieland F and Moelleken J (2006) COPI-mediated transport. *J Membr Biol* **211**:65-79.

Cramer H, Schmenger K, Heinrich K, Horstmeyer A, Boning H, Breit A, Piiper A, Lundstrom K, Müller-Esterl W and Schroeder C (2001) Coupling of endothelin receptors to the ERK/MAP kinase pathway. Roles of palmitoylation and G<sub>αq</sub>. *Eur J Biochem* **268**:5449-5459.

de Nucci G, Gryglewski RJ, Warner TD and Vane JR (1998) Receptor-mediated release of endothelium-derived relaxing factor and prostacyclin from bovine aortic endothelial cells is coupled. *Proc Natl Acad Sci USA* **85**:2334-2338.



MOL 51581

Eguchi S, Hirata Y and Marumo F (1993) Endothelin subtype B receptors are coupled to adenylate cyclase via inhibitory G protein in cultured bovine endothelial cells. *J Cardiovasc Pharmacol* **22**:S161-S163.

Fons RD, Bogert BA and Hegde RS (2003) Substrate-specific function of the translocon-associated protein complex during translocation across the ER membrane. *J Cell Biol* **160**:529-539.

Görlich D, Hartmann E, Prehn S and Rapoport TA (1992) A protein of the endoplasmic reticulum involved early in polypeptide translocation. *Nature* **357**:47-52.

Görlich D and Rapoport TA (1993) Protein translocation into proteoliposomes reconstituted from purified components of the endoplasmic reticulum membrane. *Cell* **75**:615-630.

Grisshammer R, Duckworth R and Henderson R (1993) Expression of a rat neurotensin receptor in *Escherichia coli*. *Biochem J* **295**:571-576.

Grünewald S, Haase W, Reiländer H and Michel H (1996) Glycosylation, palmitoylation, and localization of the human D2S receptor in baculovirus-infected insect cells. *Biochemistry* **35**:15149-15161.

Guan XM, Kobilka TS and Kobilka BK (1992) Enhancement of membrane insertion and function in a type IIIb membrane protein following introduction of a cleavable signal peptide. *J Biol Chem* **267**:21995-21998.

MOL 51581

Gurkan C, Stagg SM, Lapointe P and Balch WE (2006) The COPII cage: unifying principles of vesicle coat assembly. *Nat Rev Mol Cell Biol* **7**:727-738.

Hartmann E, Görlich D, Kostka S, Otto A, Kraft R, Knespel S, Burger E, Rapoport TA and Prehn S (1993) A tetrameric complex of membrane proteins in the endoplasmic reticulum. *Eur J Biochem* **214**:375-381.

Ménétre JF, Hegde RS, Aguiar M, Gygi SP, Park E, Rapoport TA, Akey CW (2008) Single copies of Sec61 and TRAP associate with a nontranslating mammalian ribosome. *Structure* **16**:1126-37.

Higy M, Junne T and Spiess M (2004) Topogenesis of membrane proteins at the endoplasmic reticulum. *Biochemistry* **43**:12716-12722.

Jungnickel B and Rapoport TA (1995) A posttargeting signal sequence recognition event in the endoplasmic reticulum membrane. *Cell* **82**:261-270.

Kempf J, Snook LA, Vonesch JL, Dahms TE, Pattus F and Massotte D (2002) Expression of the human  $\mu$  opioid receptor in a stable Sf9 cell line. *J Biotechnol* **95**:181-187.

Kim SJ, Rahbar R and Hegde RS (2001) Combinatorial control of prion protein biogenesis by the signal sequence and transmembrane domain. *J Biol Chem* **276**:26132-26140.

Kim SJ, Mitra D, Salerno JR and Hegde RS (2002) Signal sequences control gating of the protein translocation channel in a substrate-specific manner. *Dev Cell* **2**:207-217.

MOL 51581

Köchli R, Alken M, Rutz C, Krause G, Oksche A, Rosenthal W and Schülein R (2002) The signal peptide of the G protein-coupled human endothelin B receptor is necessary for translocation of the N-terminal tail across the endoplasmic reticulum membrane. *J Biol Chem* **277**:16131-16138.

Kyhse-Andersen J (1984) Electroblotting of multiple gels: a simple apparatus without buffer tank for rapid transfer of proteins from polyacrylamide to nitrocellulose. *J Biochem Biophys Methods* **10**:203-209.

Oksche A, Boese G, Horstmeyer A, Furkert J, Beyermann M, Bienert M and Rosenthal W (2000) Late endosomal/lysosomal targeting and lack of recycling of the ligand-occupied endothelin B receptor. *Mol Pharmacol* **57**:1104-1113.

Osborne AR, Rapoport TA and van den Berg B (2005) Protein translocation by the Sec61/SecY channel. *Annu Rev Cell Dev Biol* **21**:529-50.

Pankevych H, Korkhov V, Freissmuth M and Nanoff C (2003) Truncation of the A1 adenosine receptor reveals distinct roles of the membrane-proximal carboxyl terminus in receptor folding and G protein coupling. *J Biol Chem* **278**:30283-302.

Rapoport TA, Goder V, Heinrich SU, Matlack KE (2004) Membrane-protein integration and the role of the translocation channel. *Trends Cell Biol* **14**:568-75.

Robben JH, Knoers NV and Deen PM (2005) Characterization of vasopressin V2 receptor mutants in nephrogenic diabetes insipidus in a polarized cell model. *Am J Physiol Renal Physiol* **289**:F265-72.

MOL 51581

Sakurai T, Yanagisawa M, Takuwa Y, Miyazaki H, Kimura S, Goto K and Masaki T (1990)  
Cloning of a cDNA encoding a non-isopeptide-selective subtype of the endothelin receptor.  
*Nature* **348**:732-735.

Sambrook J and Russell DW (2001) *Molecular cloning: A laboratory manual*. Cold Spring Harbor Laboratory Press, Cold Spring Harbor, USA.

Schüle R, Hermosilla R, Oksche A, Dehe M, Wiesner B, Krause G and Rosenthal W (1998)  
A dileucine sequence and an upstream glutamate residue in the intracellular carboxyl terminus of the vasopressin V2 receptor are essential for cell surface transport in COS.M6 cells. *Mol Pharmacol* **54**:525-35.

Schwieger I, Lautz K, Krause E, Rosenthal W, Wiesner B and Hermosilla R (2008) Derlin-1 and p97/valosin-containing protein mediate the endoplasmic reticulum-associated degradation of human V2 vasopressin receptors. *Mol Pharmacol* **73**:697-708.

Seko T, Ito M, Kureishi Y, Okamoto R, Moriki N, Onishi K, Isaka N, Hartshorne DJ and Nakano T (2003) Activation of RhoA and inhibition of myosin phosphatase as important components in hypertension in vascular smooth muscle. *Circ Res* **92**:411-418.

Seo B, Oemar BS, Siebenmann R, von Segesser L and Luscher TF (1994) Both ETA and ETB receptors mediate contraction to endothelin-1 in human blood vessels. *Circulation* **89**:1203-1208.

MOL 51581

Shan SO and Walter P (2005) Co-translational protein targeting by the signal recognition particle. *FEBS Lett* **579**:921-926.

van den Berg B, Clemons WM Jr, Collinson I, Modis Y, Hartmann E, Harrison SC and Rapoport TA (2004) X-ray structure of a protein-conducting channel. *Nature* **427**:36-44.

von Heijne G (1985) Signal sequences. The limits of variation. *J Mol Biol* **184**:99-105.

von Heijne G (1990) Protein targeting signals. *Curr Opin Cell Biol* **2**:604-608.

Wallin E and von Heijne G (1995) Properties of N-terminal tails in G-protein coupled receptors: a statistical study. *Protein Eng* **8**:693-698.

Walter P and Johnson AE (1994) Signal sequence recognition and protein targeting to the endoplasmic reticulum membrane. *Annu Rev Cell Biol* **10**:87-119.

Wickner W and Schekman R. (2005) Protein translocation across biological membranes. *Science* **310**:1452-1456.

Wietfeld D, Heinrich N, Furkert J, Fechner K, Beyermann M, Bienert M and Berger H (2004) Regulation of the coupling to different G proteins of rat corticotropin-releasing factor receptor type 1 in human embryonic kidney 293 cells. *J Biol Chem* **279**:386-394.

MOL 51581

## Footnotes

This work was supported by grants from the Deutsche Forschungsgemeinschaft (SFB 449).

<sup>1</sup>Current affiliation : Charité – Universitätsmedizin Berlin, Biomedizinisches  
Forschungszentrum CVK, Augustenburgerplatz 1, 13353 Berlin Germany

<sup>2</sup>These authors contributed equally to this work

## Legends to figures

Fig. 1. Schematic representation of the constructs used in this study and of the N tail sequence of the ET<sub>B</sub>R. (A) Constructs (see the text for details). ET<sub>B</sub>R constructs were fused C-terminally with GFP to allow their subcellular localization. N-terminal signal peptides are indicated by black boxes, Glu<sup>28</sup>-Trp<sup>54</sup> sequences by white boxes. PrP marker protein fusions are indicated in grey. The roman numbers indicate transmembrane domains; N-glycosylation sites are indicated by a forked shape. (B) N tail sequence of the ET<sub>B</sub>R (single letter code). The signal peptide (black box) and the Glu<sup>28</sup>-Trp<sup>54</sup> sequence (white box) are indicated.

Fig. 2. Northern blot analysis of constructs ET<sub>B</sub>.GFP and ET<sub>B</sub>Δ27.GFP expressed in transiently transfected HEK 293 cells. The β actin control is shown on the lower panel. Untransfected cells (-) were used as a control for the specificity of the probe. The Northern blot is representative of three independent experiments.

Fig. 3. Pharmacological properties of ET<sub>B</sub>.GFP and ET<sub>B</sub>Δ27.GFP in transiently transfected HEK 293 cells. (A) Specific [<sup>125</sup>I]-ET1 binding profiles of intact cells. Data points represent mean values of triplicates which differed by less than 10%. Unspecific binding contributed up to 25% of total binding. The results are representative of two independent experiments. The calculated K<sub>D</sub> and B<sub>max</sub> values ± SD are indicated. (B) ET-1-mediated inositol phosphate accumulation in intact transiently transfected HEK 293 cells expressing the same constructs as in A. Data points represent mean values of triplicates (± SD). The dose response curve is representative for two independent experiments. The calculated EC<sub>50</sub> values (± SD) are indicated.

MOL 51581

Fig. 4. Glycosylation state analyses of the constructs ET<sub>B</sub>.GFP and ET<sub>B</sub>Δ27.GFP in transiently transfected HEK 293 cells. Receptors were immunoprecipitated from cell lysates using a polyclonal rabbit anti-GFP antiserum and detected by immunoblotting using a monoclonal mouse anti-GFP antibody and alkaline phosphatase-conjugated anti-mouse IgG. Receptors were left untreated (-) or treated with EndoH (EH) or PNGaseF (PF) to remove high mannose and both high mannose and complex-glycosylations respectively. Untransfected HEK 293 cells were used as a control (Co). The immunoblot is representative of three independent experiments.

Fig. 5. Subcellular location of the constructs ET<sub>B</sub>.GFP and ET<sub>B</sub>Δ27.GFP in transiently transfected HEK 293 cells. (A) Confocal LSM analyses. The GFP fluorescence signals of the receptors (green) were recorded and computer overlaid with Trypan blue plasma membrane signals (red; upper two panels) or Rhodamine 6G ER signals (red; lower two panels). The horizontal (xy) scans show representative cells. Scale bar = 10 μm. Similar data were obtained in three independent experiments. (B) Quantification and statistical analysis of the GFP fluorescence signals. The GFP signal intensities at the plasma membrane and in the cell's interior were measured and quantified using an 8 Bit grey scale (ranging from 0 to 250). Columns show the total GFP fluorescence intensity of cells ±SD (left panel, n= 30 cells) or the ratio of plasma membrane and intracellular signals ±SD (right panel, n= 30 cells).

Fig. 6. FRAP experiments using transiently transfected HEK 293 cells expressing constructs ET<sub>B</sub>.GFP and ET<sub>B</sub>Δ27.GFP. (A) Confocal LSM. Endosomal compartments containing ET<sub>B</sub>.GFP (upper panel) or ET<sub>B</sub>Δ27.GFP (lower panel) were identified by colocalizing the receptor's GFP signals with those of the cotransfected endosomal marker protein pEYFP-Endo (not shown). ROIs (white circles) were selected for the endosomal compartments and



MOL 51581

the GFP fluorescence signals were bleached with maximal laser intensity. FRAP in the ROIs was recorded over time. (B) Quantification and statistical analysis. FRAP measurements in the ROIs were performed using the LSM software. Data points represent mean values calculated from measurements of 8 cells (ET<sub>B</sub>.GFP) or 6 cells (ET<sub>B</sub>Δ27.GFP) and are expressed in percent of the initial value.

Fig. 7. Prion protein targeting assay. (A) Design of the prion protein targeting assay for the cotranslational assessment of targeting and gating functions of signal peptides; SP = signal peptide; Ri = ribosome; T = translocon. I = transmembrane domain 1. See the text for details. (B) Targeting/gating assay. Upper panel: ET<sub>B</sub>.SP.PrP and ET<sub>B</sub>.SP28.PrP were translocated and their topologies were assessed by a protease protection assay and SDS PAGE/autoradiography. The resulting protein bands are indicated and explained in the text. All samples were treated with the N glycosylation inhibitor NYT to remove N glycosylations of the prion protein moieties thereby facilitating interpretation of the results. PK = proteinase K; TX = Triton X-100. The targeting/gating assay is representative of three independent experiments. Lower panel: Schematic interpretation of the data shown in B and depiction of the resulting protein bands. PK-digested protein moieties are indicated by a cross.

Fig. 8. Molecular structure of the closed canine Sec61 protein-conducting channel. Left panel: side view; right panel: view from the cytosolic side. The lipophilic potential is indicated by a colour code (blue = hydrophilic, green/brown = hydrophobic). Spatial dimensions are indicated in Å (white arrows). A helical structure model of the signal peptide of the ET<sub>B</sub>R is inserted into the channel cavity (yellow, amino acids 6-26) above the plug segment (orange) which seals the channel (Rapoport et al., 2004). The structure was adapted from Ménétret et al. (2008) and the corresponding entry in the pdb database (code 3DKN, backbone white-gray).

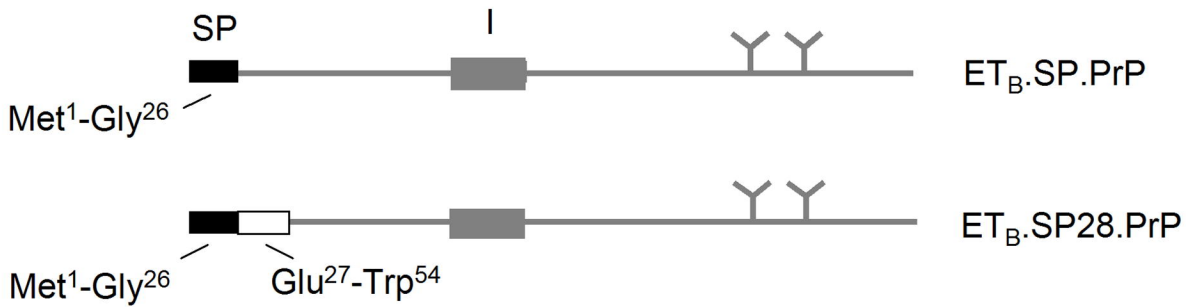
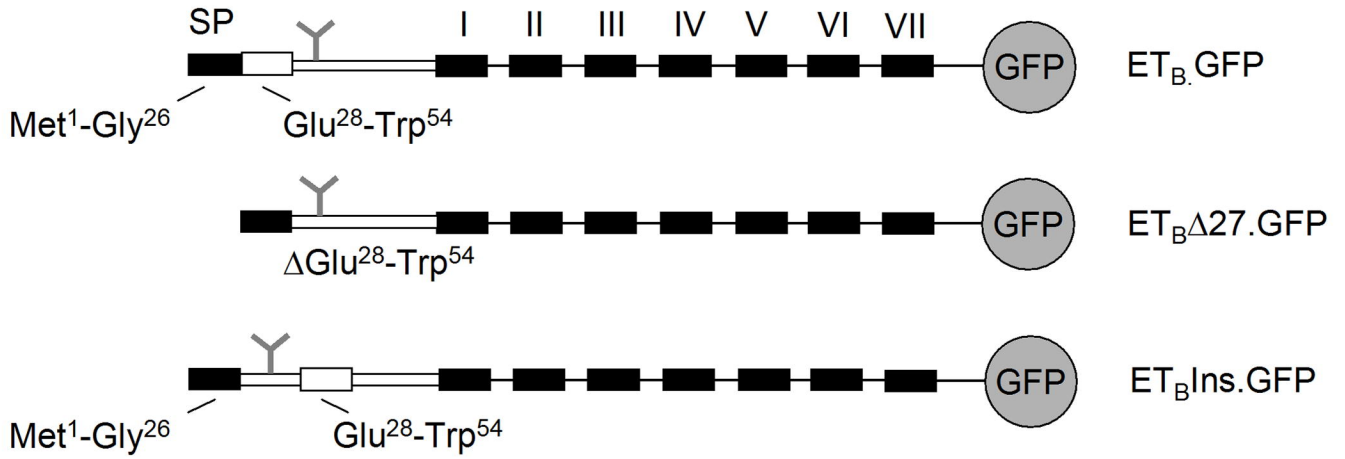
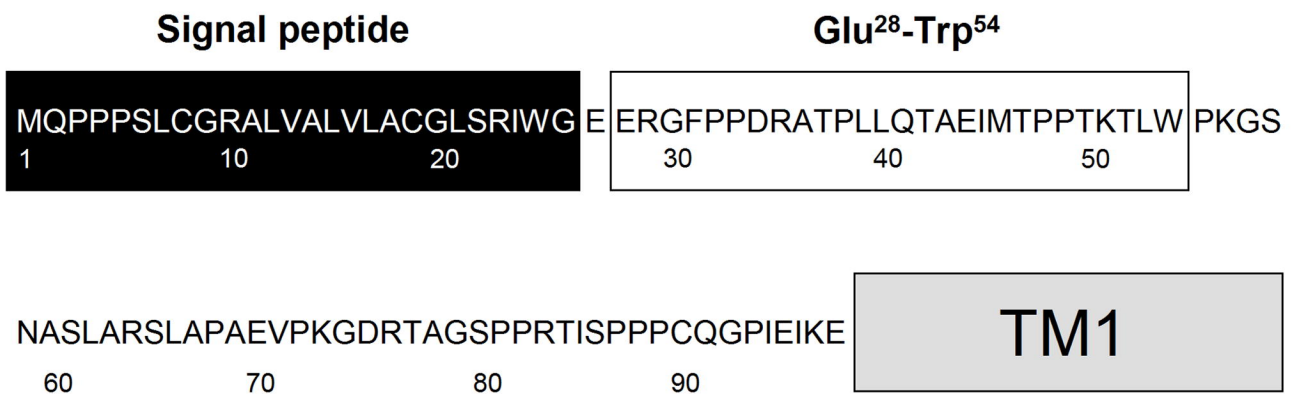
MOL 51581

Fig. 9. Properties of the mutant ET<sub>B</sub>Ins.GFP in transiently transfected HEK 293 cells. Cells transfected with ET<sub>B</sub>.GFP and ET<sub>B</sub>Δ27.GFP were used as controls. (A) Binding of saturating concentrations of [<sup>125</sup>I]-ET1 (400 pM) to intact cells. Specific binding is shown. Columns represent mean values of triplicates which differed by less than 10%. Unspecific binding contributed up to 25% of total binding. The results are representative of two independent experiments. (B) Confocal LSM: The receptor's GFP fluorescence signals (green, left panel) and the plasma membrane Trypan blue signals (red, central panel) were recorded and computer overlaid (right panel). The horizontal (xy) scans show representative cells. Scale bar = 10 μm. Similar data were obtained in three independent experiments. (C) Quantification and statistical analysis of the GFP fluorescence signals at the plasma membrane. Columns represent signal intensities ±SD measured and quantified using an 8 Bit grey scale (ranging from 0 to 250). (ET<sub>B</sub>.GFP, n = 27 cells; ET<sub>B</sub>Δ27.GFP, n = 27 cells; ET<sub>B</sub>Ins.GFP, n = 16 cells).

Fig. 10. Schematic depiction of the hairpin insertion mechanism of a signal peptide and its adjacent N tail sequence during early receptor biogenesis. Gating of the Sec61 channel (white) may be facilitated by an associated ("a"), or, in contrast, by a non-associated combination of signal peptide ("b") and adjacent sequence (light grey). In either case, signal peptide and adjacent sequence match functionally.

**Fig. 1**

Molecular Pharmacology Fast Forward. Published on January 9, 2009 as DOI: 10.1124/mol.108.051581  
 This article has not been copyedited and formatted. The final version may differ from this version.

**A****B**

**Fig. 2**

Molecular Pharmacology Fast Forward. Published on January 9, 2009 as DOI: 10.1124/mol.108.051581  
This article has not been copyedited and formatted. The final version may differ from this version.

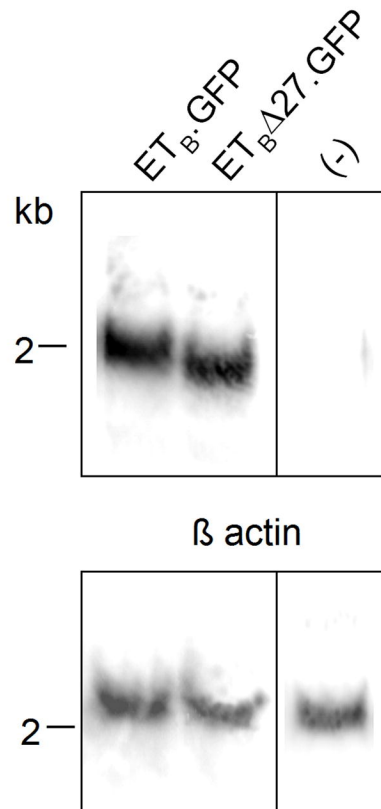
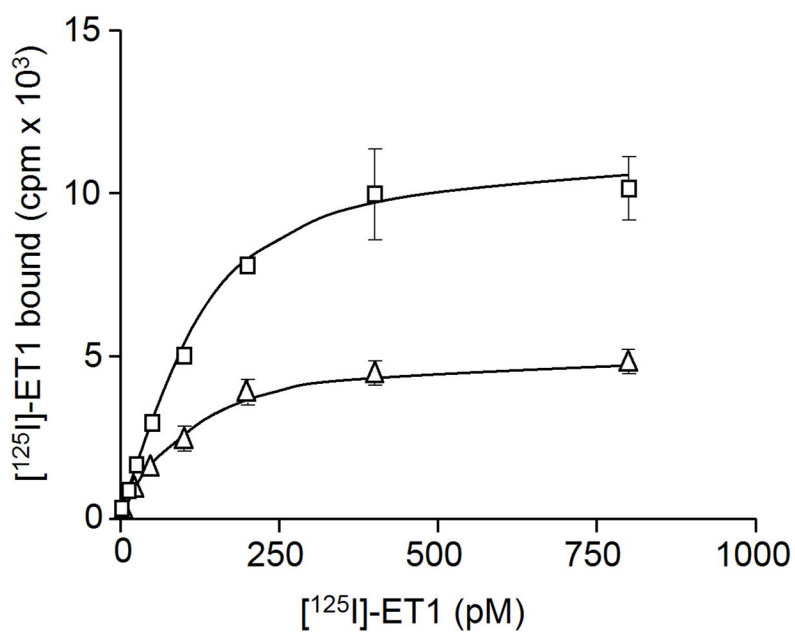


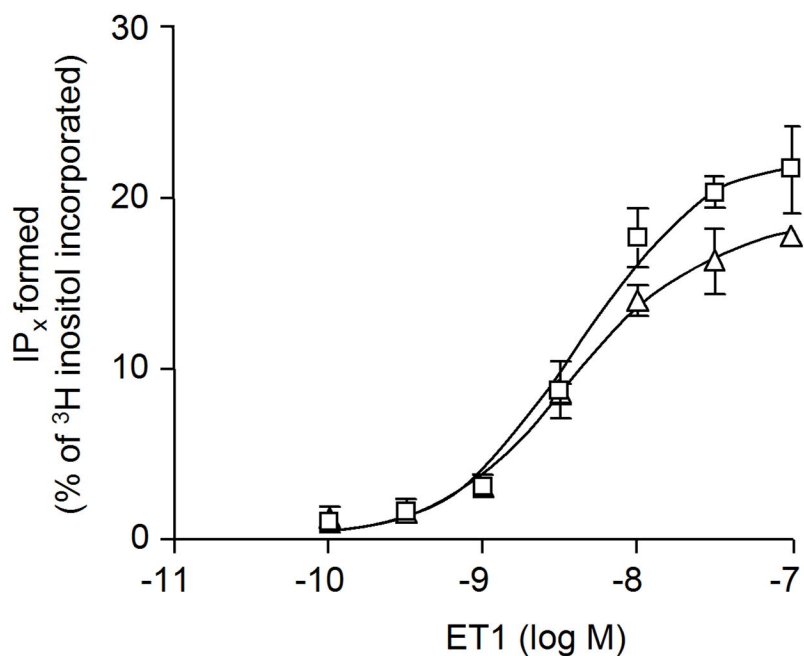
Fig. 3

A



□ ET <sub>B</sub> .GFP K <sub>D</sub> = 0.14±0.02 nM B <sub>max</sub> = 84.5±9.2 fmol/mg	△ ET <sub>B</sub> Δ27.GFP K <sub>D</sub> = 0.13±0.02 nM B <sub>max</sub> = 38.1±4.9 fmol/mg
--	---

B



□ ET <sub>B</sub> .GFP EC <sub>50</sub> = 4.5±0.1 nM	△ ET <sub>B</sub> Δ27.GFP EC <sub>50</sub> = 3.3±0.1 nM
---	--

**Fig. 4**

Molecular Pharmacology Fast Forward. Published on January 9, 2009 as DOI: 10.1124/mol.108.051581  
This article has not been copyedited and formatted. The final version may differ from this version.

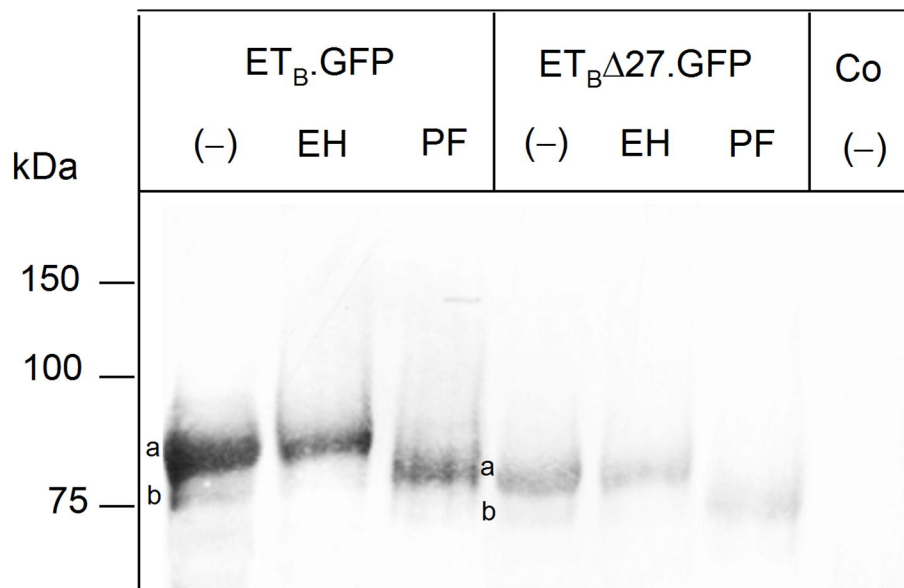
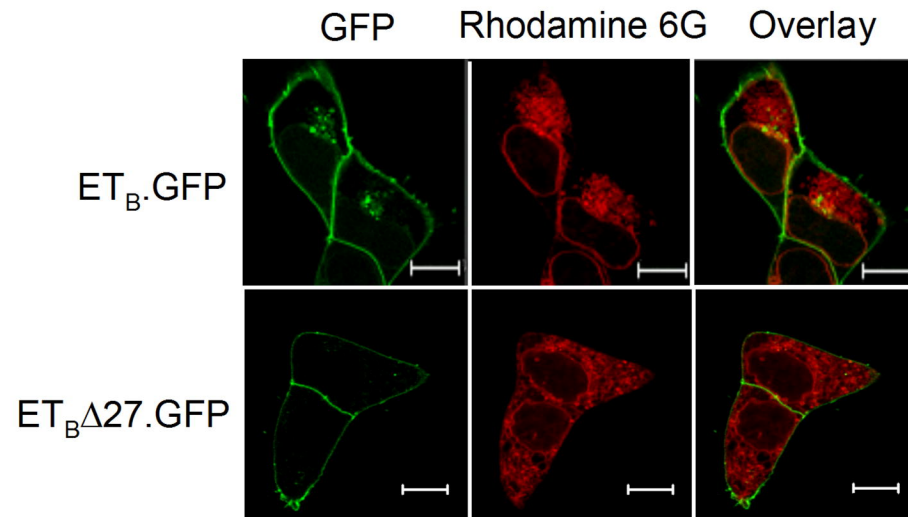
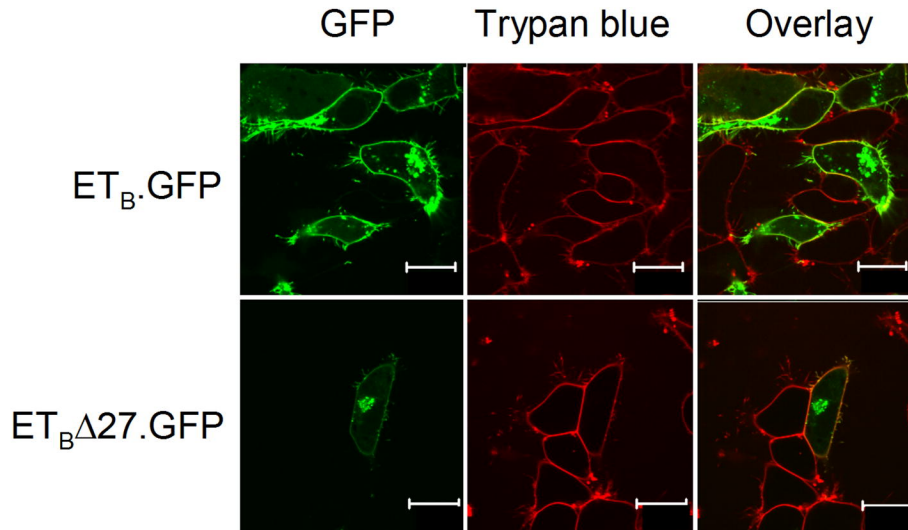
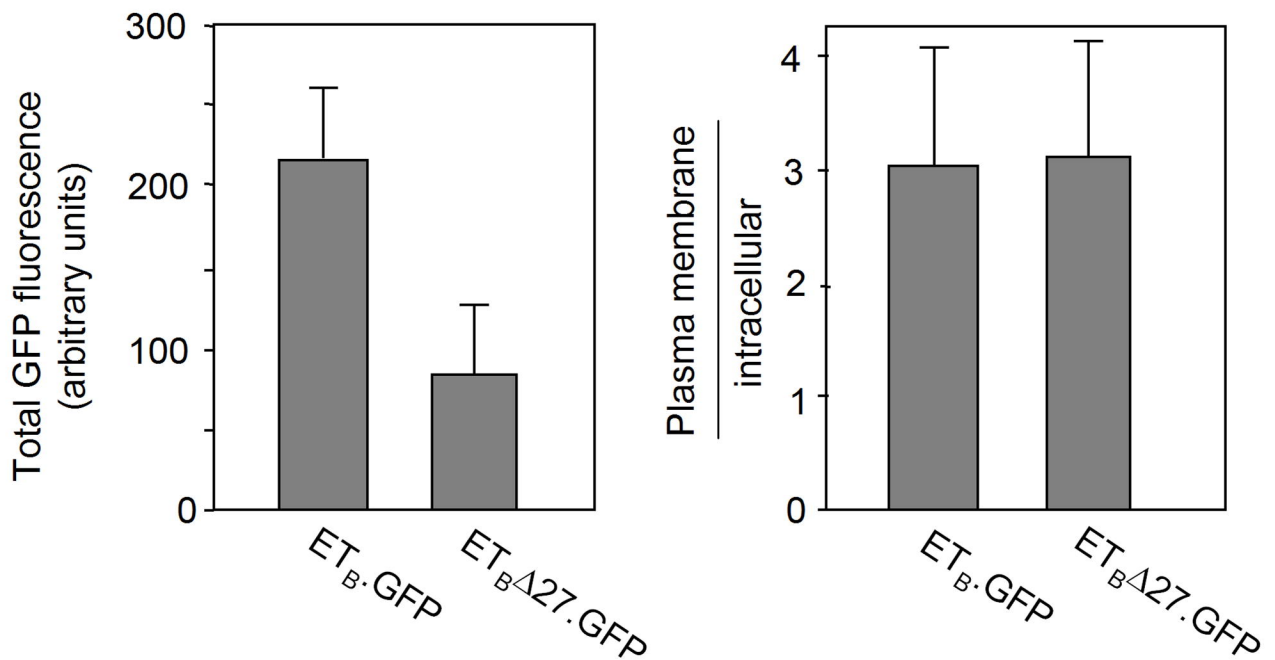


Fig. 5

**A**



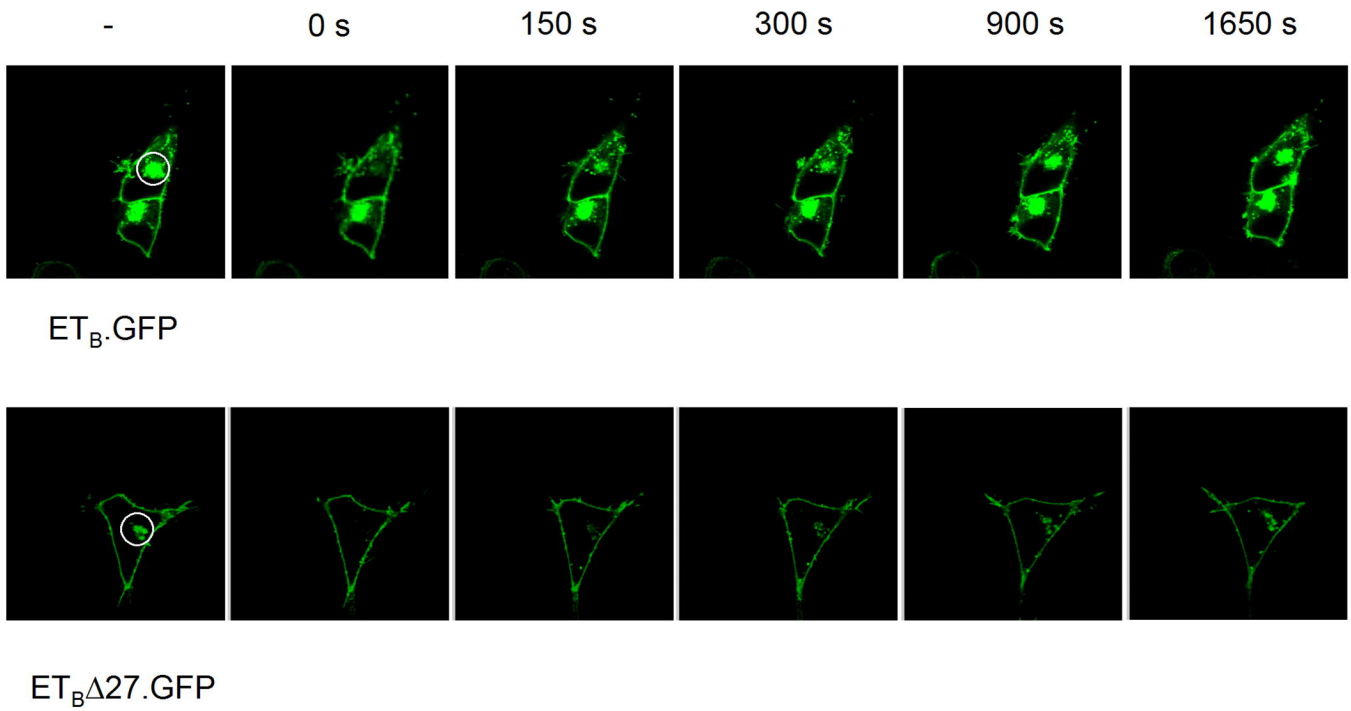
**B**



**Fig. 6**

Molecular Pharmacology Fast Forward. Published on January 9, 2009 as DOI: 10.1124/mol.108.051581  
This article has not been copyedited and formatted. The final version may differ from this version.

**A**



**B**

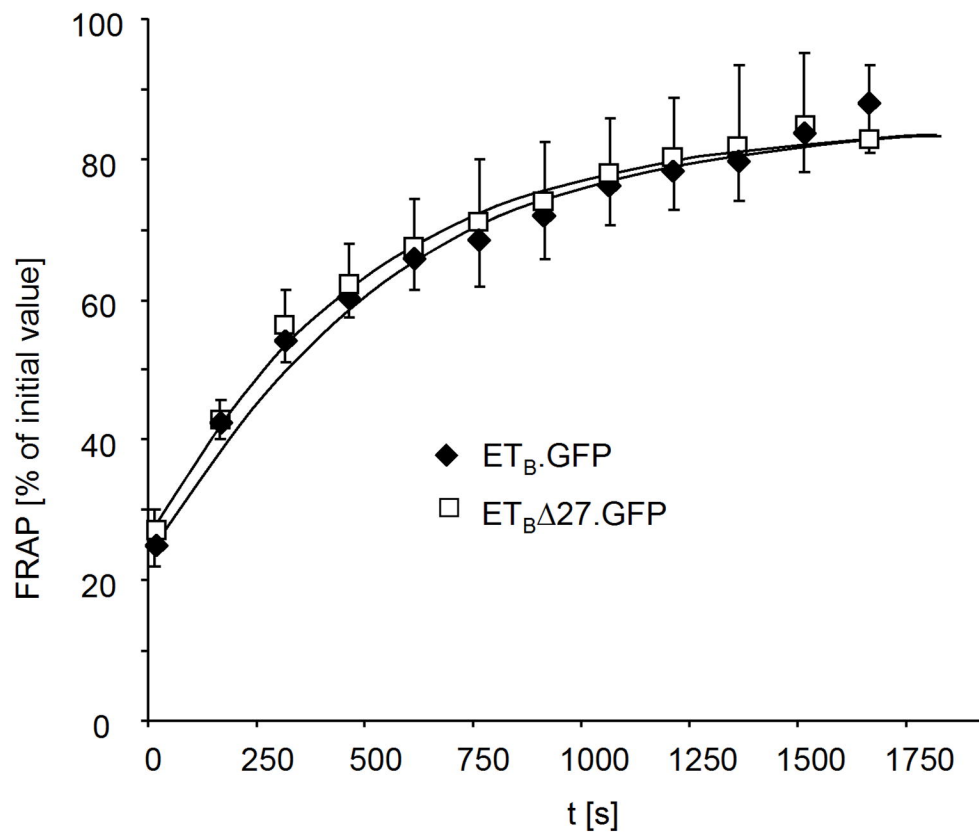
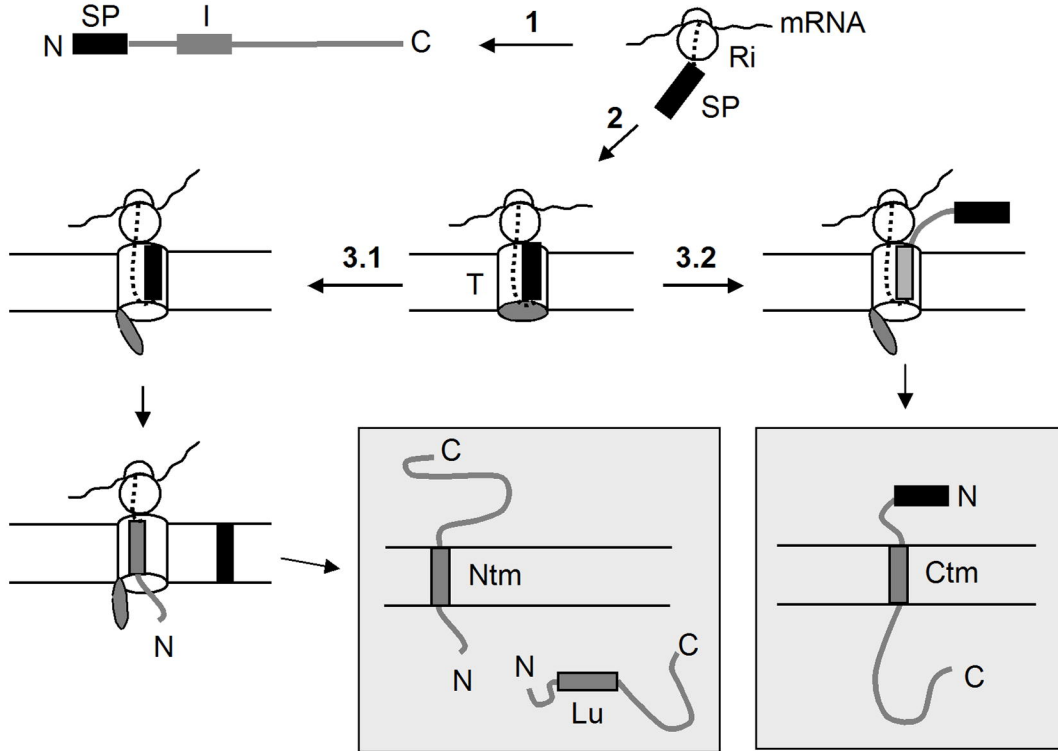




Fig. 7

**A**



**B**

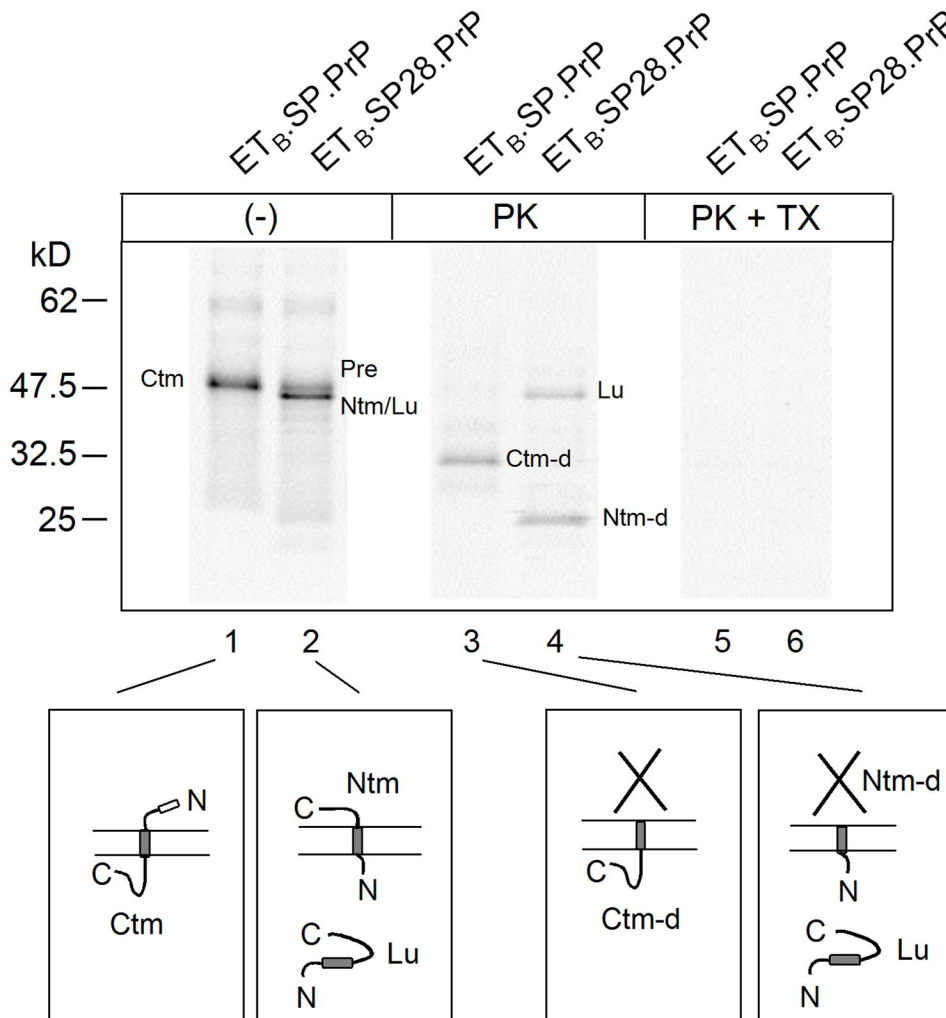
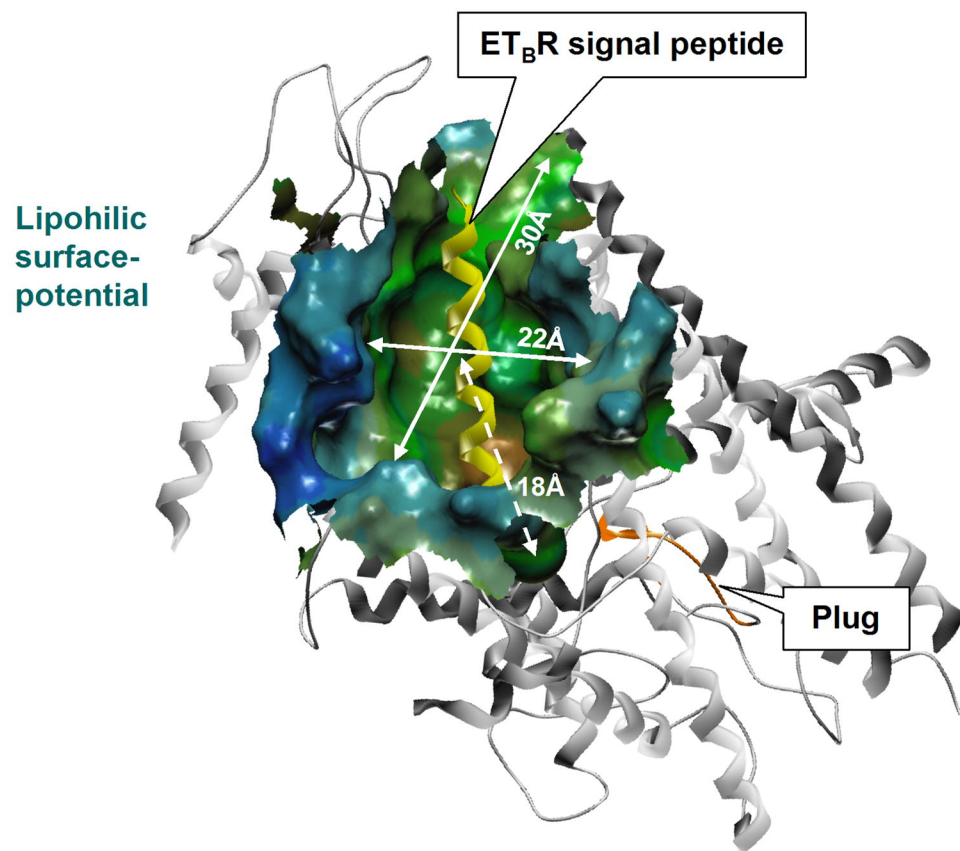
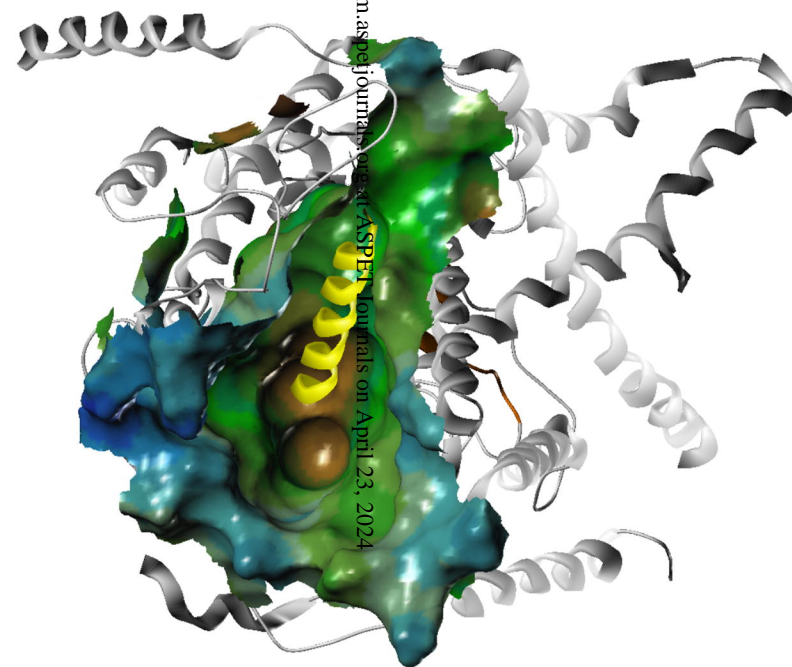


Fig. 8

Side view



View from the cytosolic side



**Fig. 9**

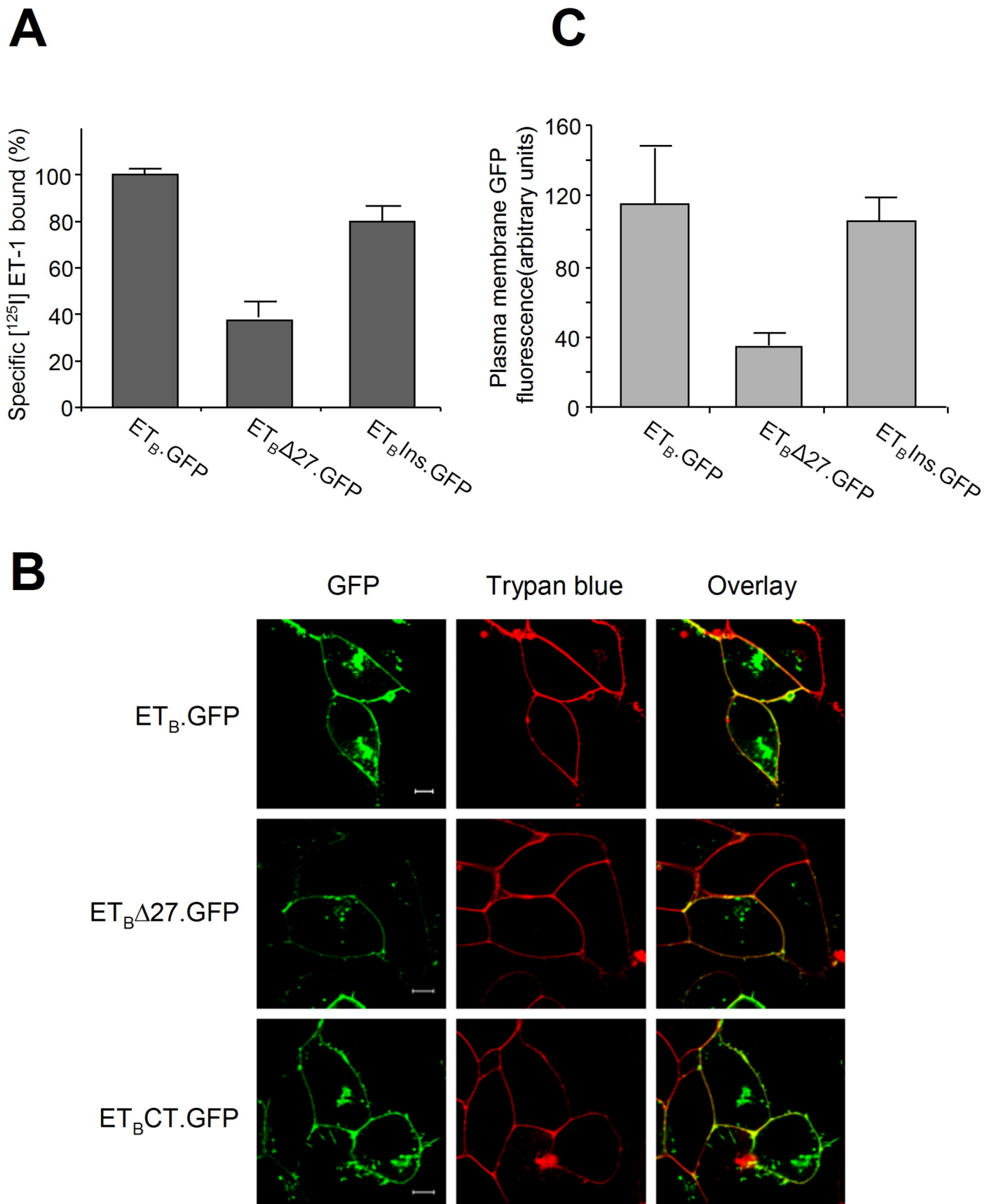


**Fig. 10**

Molecular Pharmacology Fast Forward. Published on January 9, 2009 as DOI: 10.1124/mol.108.051581  
This article has not been copyedited and formatted. The final version may differ from this version.

